Optimization of Catalyst Nano-structures through Alloying and De-alloying Process---Research on Ag-Co Catalyst for Catalytic Oxygen Reduction in Alkaline Media

Rongzhong Jiang, Deryn Chu, Joshua P. McClure, and Dat T. Tran

Sensors and Electron Devices Directorate, U.S. Army Research Laboratory

2800 Powder Mill Road, Adelphi, MD 20783-1197. Email: Rongzhong.jiang.civ@mail.mil, Phone: +1 301-394-0295, Fax: +1 301-394-0273

ABSTRACT

A highly active and durable Ag-Co catalyst was synthesized by optimizing the catalyst nano-structures for realization of fast electron-transfer and ion-transfer. De-alloying process was used to remove excess of cobalt in Ag-Co sample and form nano-dendrimers. The activity of the Ag-Co materials is dependent on the Co content; and the Co/Ag ratio in 0.10 (a/a) gives the best performance for oxygen reduction reaction (ORR). Further enhancement of activity is achieved by addition of graphene nano-platelets (GNP) as a catalyst support into the Ag-Co material, and followed by a process of heat-treatment. Oxygen reduction at the Ag-Co nano-catalyst belongs to a 4-electron reaction process to produce water in alkaline media. Finally, the catalytic activity was compared with a commercially available Ag nano material (20 – 40 nm). There is a 170 mV decrease in over potential; and 6-times enhancement in current density at 0.75V (versus RHE) and 1600 rpm rotation rate for ORR in oxygen saturated 0.1M KOH solution.

Keywords: Catalyst nanostructure, ORR, Ag-Co, graphene nano-platelets, Heat-treatment.

1 INTRODUCTION

The state of the art catalysts for fuel cell are expensive noble metals, including platinum black and platinum-based metal alloys. For a polymer electrolyte membrane fuel cell (PEMFC), the catalyst covers about 60% of the cost of a fuel cell stack in automobile application [1]. The quest for more efficient fuel cell technologies necessitates the development of low cost, highly active and stable catalyst materials. The fast improvement of catalytic activity in recent years is benefit from the emerging of nanotechnology for material synthesis and processing [2-4], such as carbon nanotube, nanofiber, mesoporous carbon], and graphene. These nano materials can either be used as a catalyst support or directly used as a catalyst. In recent years, a lot of nano-structured noble metals and alloys [5-8], such as metal nanoparticles, nanowires, nanoframes, nanohollows, and nano-coreshells, have been successfully synthesized, and tested for fuel cell catalysts. Optimization of particle size and particle's nano-structure at the atomic level can precisely and effectively tune catalytic properties of materials, and enabling enhancement in both catalytic activity and stability. It is well known that silver is used for catalytic oxygen reduction in alkaline media [9-10]. The cost of silver is around 1% of Pt, and the abundance of it is approximately 1500% of Pt. After alloying with transition metals, such as Co, it gives better catalytic activity [11]. Holewinski et al [12] synthesized an Ag-Co surface alloy nano particles at high temperature (500 °C), having activity around fivefold improvement over pure silver nanoparticles. In this article we report a different approach to synthesize Ag-Co nanoparticles at low temperature. Interestingly, we obtained Ag-Co nano-dendrimers by precisely controlling the size, shape, architecture, and composition. The dendritic nanoparticles showed much higher activity and stability than pure Ag nano particles for catalytic oxygen reduction reaction (ORR) in alkaline media.

2 EXPERIMENTAL

2.1 Synthesis of nanostructured catalysts

Graphene nano-platelets (GNP) with a BET surface area between 600 – 650 m^2/g were purchased from Cheap Tubes Inc. Some commercially available catalysts were purchased from Johnson Matthey, including 40% Pt nano catalyst supported on 60% active carbon (JM's 40% PtC), and Ag-nanopowder (JM's Ag-nano, particle size 20–40 nm). Nano-structured Ag-Co was synthesized by reducing a mixture of silver and cobalt compounds in the presence of GNP. Silver ammonia complex was formed by adding ~ 1g $AgNO_3$ and 5 ml ammonia hydroxide, and moved in a 250 ml flask containing 80 ml water. On the other hand, different quantity of $CoC_2O_4 \cdot 2H_2O$ was suspended in 40 ml water and 5 ml ammonia hydroxide, and moved in the same flask. The reducing reagent was $NaBH_4$ solution by dissolving $NaBH_4$ in 40 ml water. The Ag-Co was synthesized by slowly dropping $NaBH_4$ solution into the flask and fast stirring. The amount of Co in the Ag-Co alloy was adjusted by a de-alloying process in 1M HCl and controlling Co/Ag ratio by a specific time period. The Ag content in the Ag-Co alloy was determined by gravimetrical analysis, in which hydrochloric acid was used to thoroughly remove the cobalt existed in the Ag-Co alloy, and weighting the dry Ag powder. The pure Ag fine power was synthesized with the same method of making Ag-Co but without adding cobalt oxalate in the reaction solution. GNP supported Ag-Co (Ag-Co/GNP) was synthesized with the same method of making Ag-Co and controlling Co/Ag atomic ratio 0.10. A quantitative amount of GNP was added

in the reaction solution before dropping $NaBH_4$ solution in the flask. The Ag-Co/GNP contained 30% Ag-Co alloy and 70% GNP. The Ag-Co/GNP was further heat-treated to enhance the catalytic activity at 500 °C in argon atmosphere. We called the heat-treated catalyst as HT-Ag-Co/GNP.

2.2 Instrumental Analysis

Transmission electron microscope (TEM) was obtained with a high-resolution JEOL 2100 FE instrument equipped with an EDAX X-ray detector. Selected area electron diffraction (SAED) patterns and energy-dispersive X-ray spectroscopy (EDS) analyses were also obtained during the measurements. Scanning electron microscope (SEM) image was obtained with FEI QUANTA 200F instrument.

X-Ray diffraction analysis (XRD) results were obtained from a Rigaku Ultima III instrument with Cu Kα radiation (λ = 1.5418 Å) using a Bragg-Brentano Configuration. The measurements were conducted with scan rate of 1.0 degree (2θ) per minute and each diffraction data point was collected at the interval of 0.02 degree (2θ) for the total spectrum range of 10 to 90 degree (2θ).

2.3 Electrochemical Analysis

A Pine Bipotentiostat RDE4 was used for electrochemically analyzing the synthesized catalysts by depositing the catalyst samples from ink mixtures onto a glassy carbon (GC) disk electrode. The catalyst ink in 1:1 water/1-propanol solution was prepared by ultrasonically treatment with a Branson Sonifier 450 at a duty cycle 40 and out-put control 8 for 10 minutes. The final content of Ag or Ag-Co ink was 4 mg/ml after excluding the mass of supporting GNP. Next, 5 μl of catalyst ink was coated on the GC disk working electrode (0.196 cm^2), and dried at 40°C for ~60 minutes. The final coating on the GC disk electrode contained 95% total catalyst and 5% Nafion with an Ag or Ag-Co loading of 0.1 mg/cm^2. The inks for JM's 40% PtC and JM's Ag-nano were prepared separately with the same procedures. The final coating on the GC electrode was 95% Nafion and 5% catalyst with a Pt loading 0.02 mg/cm^2, and Ag loading 0.10 mg/cm^2. All voltammetrical experiments were performed in argon (Ar.) or O_2 saturated 0.1M potassium hydroxide (KOH) solution at room temperature (20 ± 1°C). A three electrode glass cell was used for electrochemical study containing three compartments separated by a porous ceramic layer. A platinum wire counter electrode and a saturated calomel reference electrode (SCE) were used in the cell. The experimental results are reported based on reversible hydrogen electrode (RHE).

3 RESULTS AND DISCUSSION

3.1 TEM and SEM results

Fig. 1 shows TEM and SEM images of various catalysts obtained by chemical synthesis. The particle size of Ag-Co is significantly reduced in comparison of pure Ag without alloying, although they are synthesized in the same experimental conditions. The particles of graphene supported Ag-Co/GNP are dispersed on the large surface of GNP. After heat-treatment, the particles of HT-Ag-Co/GNP seem embedded in the GNP, and less Ag-Co particles can be seen. Interestingly, the unsupported Ag-Co looks like a dendritic material, where the particles are first joined together to form short wires, and then, the wires are connected to form dendrimers. The SAED image indicates that the dendrimers have good crystal structure, which is judged from the multiple clear rings and the bright dots on the rings in the dark field. The Ag and Co elements are detected by EDS analysis (not shown in the figure). The elemental maps (also not shown in the figure) demonstrate a uniform distribution of Ag and Co. The elemental map of Co has the same shape with that of the Ag, which is an evidence of Ag-Co alloy, instead of an Ag and Co mixture.

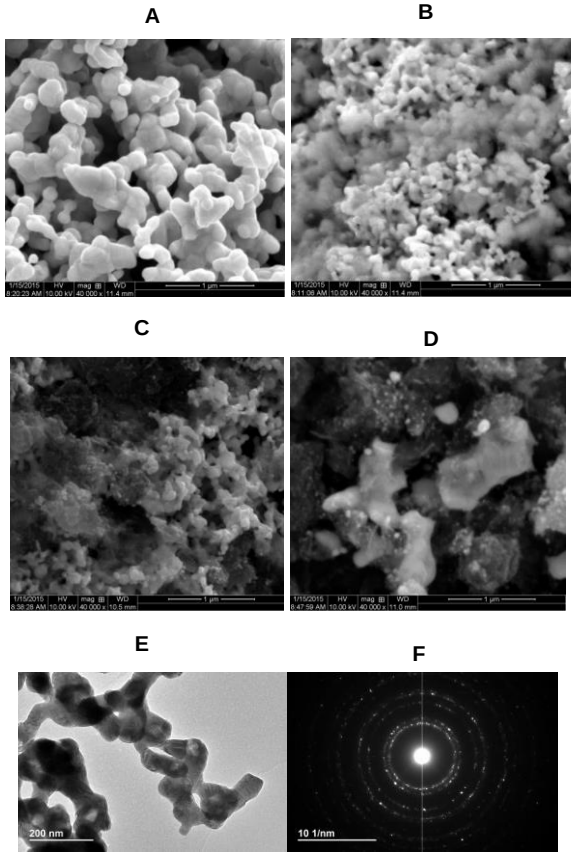

Fig.1 TEM and SEM images of nanostructured catalysts prepared at different conditions. A. SEM of Ag-nano particles by chemical synthesis; (B) SEM of Ag-Co with Co/Ag ratio 0.10 (atomic); (C) GNP (70%) supported Ag-Co (30%, Co/Ag=0.10); D. HT-Ag-Co/GNP (HT at 500 °C); (E) TEM of Ag-Co (Co/Ag = 0.10); and (F) SAED of Ag-Co.

3.2. XRD results

Fig. 2A shows XRD patterns of unsupported Ag-Co alloys with different Co/Ag atomic ratios. Five typical peaks of pure Ag can be seen. When Ag is alloyed with Co, the positions of these peaks have only a slight movement; but all of the peaks become wider. The parameters of the highest peak with Miller index at plane (111) are examined. With increasing the content of Co in the alloy, the half-wave width of the peaks increases, which is a sign of decrease in crystallite size; and the peak position moves to higher degree (2θ). Simultaneously, the perpendicular distance between adjacent lattice planes (d-spacing) becomes decreased, which implies that the Ag lattice structure shrinks after alloying with Co. The shrink in Ag lattice structure may cause a defect of Ag crystal, and change the catalytic property. Fig. 2B shows XRD pattern of Ag-Co supported on GNP. The GNP was introduced in the synthetic process. A small new peak appears at 26.76 degree (2θ) for Ag-Co/GNP, which is a typical peak of graphite structure. For the Ag-Co/GNP, the peak position at plane (111) further increases to higher 2θ value, and lower d-spacing.

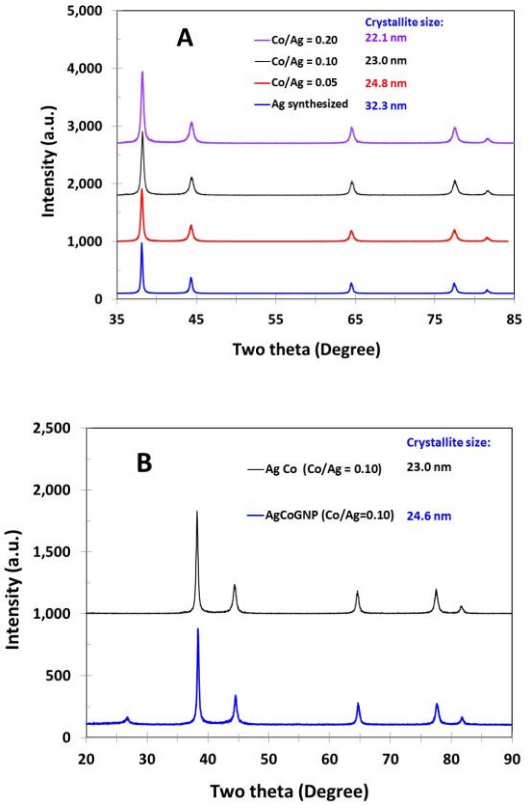

Fig. 2 XRD patterns of various catalysts. (A) XRD of Ag-Co with different Co/Ag ratios; and (B) XRD of Ag-Co with and without GNP support.

3.3 Electrochemical results

The activity of original Ag-Co alloy was not satisfied. Higher activity was achieved by a de-alloying process acidic solution to remove excess of cobalt in the Ag-Co.

Fig. 3 shows electrochemical behaviors of Ag-Co coated electrodes and their catalytic activity for oxygen reduction. In argon saturated solution (Fig. 3A), the oxygen was removed from the electrolyte; and the cyclic voltammograms (CVs) show typical electrochemcial surface waves. The original Ag-Co alloy has a small cathodic peak and two small anodic peaks. After de-alloyed, only one anodic peak is seen; and both the cathodic and anodic peaks become about two times larger. About 70–100 mV positive potential shift is observed versus pure Ag nano catalyst (JM's Ag-nano). The catalytic activity was measured with a rotating disk electrode in O_2 saturated electrolyte solution (Fig. 3B). The highest catalytic activity was obtained from the de-alloyed Ag-Co catalyst, and its polarization curve has the most positive half-wave potential (0.74V vs. RHE). Unfortunately, the Co content in the de-alloyed Ag-Co is difficult to control accurately. Therefore, we changed the Co content in the synthetic process by more accurately control the Co/Ag ratio. When the Co/Ag atomic ratio as 0.10, the best activity was obtained, which has the same electrochemical performance as that of the de-alloyed Ag-Co.

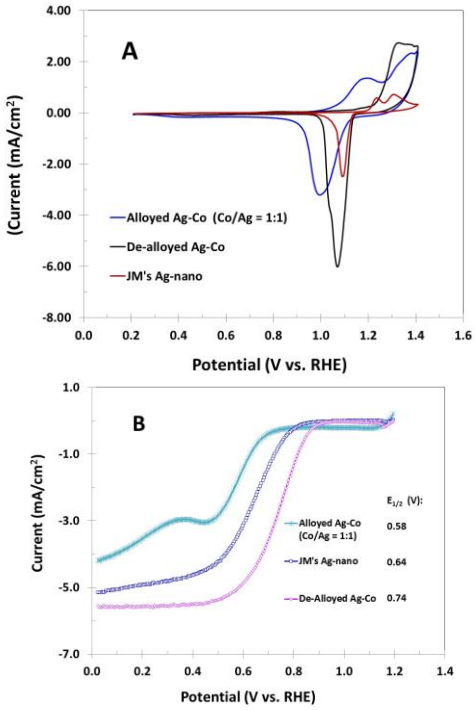

Fig. 3. Electrochemical behaviors of Ag-Co coated electrodes and their catalytic activity for oxygen reduction. 10 mV/s. 1600 rpm. (A) Cyclic voltammograms in argon saturated 0.1M KOH; (B) Polarization curves in O_2 saturated 0.1M KOH;

Further enhancement of activity is achieved by addition of graphene nano-platelets (GNP) as a catalyst support into the Ag-Co material, and followed by a process of heat-treatment. The performance of the best catalyst is evaluated

by comparison with commercially available catalysts. Fig.4A shows polarization curves of HT-Ag-Co/GNP and some commercial catalysts coated electrodes for catalytic oxygen reduction. In comparison of JM's Ag-nano, the HT-Ag-Co/GNP catalyst has raised 170 mV in half wave potential. In comparison of JM's 40% PtC, the HT-Ag-Co/GNP catalyst has only 20 mV lower in half wave potential. Fig. 4B shows Tafel plots of the polarization curves. The HT-Ag-Co/GNP catalyst has even lower Tafel slope than that of the JM's PtC. The quantitative comparison of catalytic activity for a series of catalysts is shown in Fig. 4C. There is 170 mV decrease in half wave potential, and 6 times improvement in current density at 0.75V (vs. RHE).

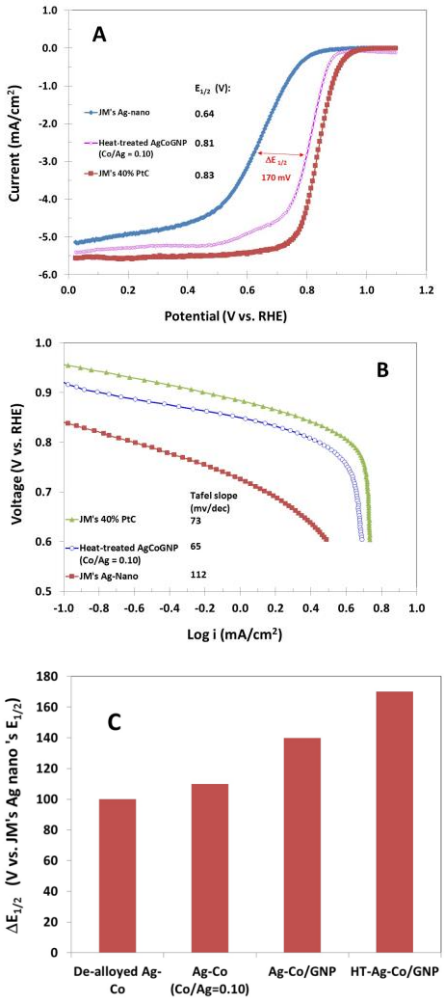

Fig. 4 (A) Polarization curves of HT-Ag-Co/GNP catalyst and commercial catalysts coated electrodes in O_2 saturated 0.1M KOH. 10 mv/s, 1600 rpm. (B) Tafel plots of the data in A. (C) Comparison of catalytic activity versus JM's Ag nano-particles (20-30 μm).

REFERENCES

[1] Marcinkoski, J.; James, B. D.; Kalinoski, J. A.; Podolski, W.; Benjamin, T.; Kopasz, J., "Manufacturing process assumptions used in fuel cell system cost anal-yses", J. Power Sources, 196, 5282–5292, 2011.

[2] Ebbesen, T. W.; Ajayan, P. M., "Large-scale synthesis of carbon nanotubes", Nature, 358, 220-222, 1992.

[3] Che, G. L.; Lakshmi, B. B.; Fisher, E. R.; Martin, C. R., "Carbon nanotube membrane for electrochemical energy storage and production", Nature 8, 393, 346-349, 1998.

[4] Andersen, S. M.; Borghei, M.; Lund, P.; Elina, Y. R.; Pasanen, A. Esko Kauppinen, E.; Ruiz, V.; Kauranen, P.; Skou, E. M., "Durability of carbon nanofiber (CNF) & carbon nanotube (CNT) as catalyst support for Proton Exchange Mem-brane Fuel Cells" Solid State Ionics, 3, 231, 94–101, 2013.

[5] Rong, C.; Jiang, R. Z.; Sarney, W.; Chu, D., "Ultrasound-assisted microemulsion for synthesis of Pt and PtCo nano-particles", Electrochimica Acta, 55, 6872–6878, 2010

[6] Chen, C; Kang, Y. J.; Huo, Z. Y.; Zhu, Z. W.; Wenyu Huang, W. Y.; Xin, H. L.; Snyder, J. D.; Li, D. G.; Herron, J. A.; Mavrikakis, M.; Chi, M. F.; More, K. L.; Li, Y. D.; Markovic, N. M.; Gabor A. Somorjai, G. A.; Yang, P. D.; Stamen-kovic, V. R., "Highly Crystalline Multimetallic Nanoframes with Three-Dimensional Electrocatalytic Surfaces", Science, 343, 1339-1343, 2014.

[7] Chen, H. M.; Liu, R. S.; Lo, M. Y. Chang, S. H.; Tsai, L D.; Peng, Y. M.; Lee, J. F., "Hollow Platinum Spheres with Nano-Channels: Synthesis and Enhanced Catal-ysis for Oxygen Reduction", J. Phys. Chem. C , 112, 7522–7526, 2008.

[8] Tuaev,X.; Rudi, S.; Petkov, V.; Hoell, A.; Strasser, P., "In Situ Study of Atomic Structure Trans-formations of Pt-Ni Nanoparticle Catalysts during Electrochemical Potential Cycling", ACS Nano 2013, 7, 5666–5674, 2013.

[9] Beer, S. Z.; Sandier, Y. L., "Oxygen Reduction at Silver and Silver Based Alloy Electrodes", J. Electrochem. Soc., 112, 1133, 1965.

[10] Yang Y. F.; Zhou, Y. H., "Particle size ef-fects for oxygen reduction on dispersed silver + carbon electrodes in alkaline solution", J. Electroanal. Chem., 397, 271, 1995.

[11] Lima, F. H. B.; de Castro, J. F. R.; Tician-elli, E. A., "Silver-cobalt bimetallic parti-cles for oxygen reduction in alkaline me-dia", J. Power Sources 2006, 161, 806–812.

[12] Holewinski, A.; Idrobo, J. C.; Linic, S., "High-performance Ag–Co alloy catalysts for electrochemical oxygen reduction", Nature Chemistry, 6, 828-834, 2014.